Lateralized neural mechanisms underlying the modulation of response inhibition processes

Sebastian Ocklenburg *, Onur Güntürkün, Christian Beste

Institute of Cognitive Neuroscience, Biopsychology, Department of Psychology, Ruhr-University of Bochum, Germany

ABSTRACT

Functional cerebral asymmetries (FCAs) are an important modulator of cognitive functions. Here, we investigated the temporal and spectral dynamics as well as the cortical networks underlying the lateralized modulation of executive functions related to response inhibition. To this end, we recorded event-related potentials (ERPs) during tachistoscopic presentation of verbal 'Go' and 'Nogo' stimuli in the left (LVF) and the right visual field (RVF).

Participants committed fewer false alarms to verbal Nogo stimuli presented in the RVF than to stimuli presented in the LVF. This asymmetry was paralleled by neurophysiological data. The Nogo-N2 and related delta frequency band power were stronger when response inhibition was driven by stimuli presented in the LVF, implying a stronger response conflict. This effect was mediated by stronger activations in bilateral medial-prefrontal and especially left parietal networks. This shows that asymmetries in behavioural performance do not necessarily reflect differences in the overall capability of one hemisphere to solve a task. Even though information is initially confined to one hemisphere after tachistoscopic presentation, this does not primarily cause behavioural asymmetries. Instead, hemispheric dominances in information processing can induce differences in demands on cognitive processes operating via bilateral networks that ultimately drive behavioural asymmetries.

© 2011 Elsevier Inc. All rights reserved.

Introduction

The inhibition of prepotent responses is an important instance of action selection processes and is mediated by basal ganglia and prefrontal cortical structures (e.g. Beste et al., 2010a; Chudasama and Robbins, 2006). Response inhibition is commonly assessed with Go/Nogo task. In these tasks, response inhibition is driven by different types of stimuli. Participants are asked to respond to one of the stimuli (Go) by pressing a key, whereas they have to refrain from responding when the other stimulus (Nogo) is presented (e.g. Garavan et al., 2002; Falkenstein, 2006). In this respect response inhibition performance, as well as the efficacy of executive functions in general, is influenced by information processing in the bottom-up channel (e.g. Knudsen, 2007). However, depending on the nature of stimuli, one hemisphere is more efficient in processing than the other (Hugdahl, 2000). A well-known example for these functional cerebral asymmetries (FCAs) is the relative dominance of the left hemisphere for processing of verbal stimuli in most individuals (e.g. Hugdahl, 2000; Corballis, 2003; Hirnstein et al., 2008; Westerhausen and Hugdahl, 2008). On a purely behavioural level, Measso and Zaidel (1990) showed that

FCAs influence response inhibition performance. They observed a right visual field (RVF) advantage for response inhibition accuracy, reflecting a left-hemispheric dominance for the processing of verbal stimuli (Measso and Zaidel, 1990). However, the temporal and neuronal dynamics of brain areas underlying the modulation of response inhibition processes by FCAs are elusive so far, but are most essential in developing models how asymmetries modulate executive functions. To investigate these processes, event-related potentials (ERPs) provide a powerful tool to examine various aspects of the neurophysiology underlying the modulation of response inhibition by FCAs.

In ERP studies, two components supposed to reflect different sub-processes of response inhibition are typically observed: The Nogo-N2 and the Nogo-P3 (Falkenstein et al., 1999; Bokura et al., 2001). The Nogo-N2 is supposed to reflect either pre-motor inhibition (Falkenstein et al., 1999) or response conflict (Nieuwenhuis et al., 2003). For example, Nieuwenhuis et al. (2003) investigated response inhibition in a Go/Nogo task, in which the relative frequency of Go and Nogo-stimuli was varied. Consistent with the conflict hypothesis, the N2 was observed on both Go and Nogo trials and was augmented for rare stimuli, irrespective of whether these stimuli were associated with generation or inhibition of a response. The Nogo-P3 seems to be related to the evaluation of successful inhibitory processes (Band and van Boxtel, 1999; Roche et al., 2005; Beste et al., 2008a, 2009a). This interpretation is due to the fact, that the P3 peaks too late after the

* Corresponding author at: Abteilung Biopsychologie, Institut für Kognitive Neurowissenschaft, Fakultät für Psychologie, Ruhr-Universität Bochum, Universitätsstraße 150, 44780 Bochum, Germany. Fax: +49 234 32 14377.

E-mail address: sebastian.ocklenburg@rub.de (S. Ocklenburg).

reaction itself to directly reflect response inhibition: For example, Roche et al. (2005) found that the P3 occurred over 100 ms after the mean response latency in a Go/Nogo task.

In order to investigate how FCAs affect the efficacy of response inhibition processes we compared response inhibition processes driven by verbal stimuli presented in the RVF against left visual field (LVF) presentation of the same stimuli. The Nogo-N2 and Nogo-P3 should be affected by FCA-dependent differences in the efficacy of response inhibition. Consequently, brain regions that have been linked to the Nogo-N2 and Nogo-P3, like the anterior cingulate cortex (ACC) (van Veen and Carter, 2002; Nieuwenhuis et al., 2003; Ridderinkhof et al., 2004b; Bekker et al., 2005; Beste et al., 2008a; Wascher and Beste, 2010; Beste et al., 2009b), the pre-supplementary motor area (pre-SMA, BA6) (Rushworth et al., 2004) as well as the superior and inferior frontal cortex (Konishi et al., 1998; Beste et al., 2008b) may show FCA-dependent activation differences. Interestingly, some evidence suggests that in cases with elevated demands on conflict processing capacities, the superior and inferior parietal cortex (i.e., BA7 and BA40) (Gothelf et al., 2007) are additionally recruited. Thus, response inhibition processes reflected by the Nogo-N2 may also show FCA-dependent activation differences in these brain areas.

Aside from ERP components, processes of neural oscillations are assumed to provide important insights into neuronal mechanisms underlying modulations of cognitive functions (e.g. Varela et al., 2001; Roach and Mathalon, 2008; Sauseng and Klimesch, 2008). For cognitive control processes (i.e., error monitoring) time–frequency analyses have shown that especially oscillations in the delta frequency band are empowered in cases, where demands on cognitive control and behavioural monitoring are increased (e.g. Yordanova et al., 2004; Beste et al., 2007, 2010b). In addition, plenty of evidence suggests that the alpha frequency band may also be relevant for the cognitive processes assessed in the present study. In particular, these studies have shown that a large resting or reference alpha power is positively associated with performance (Doppelmayr et al., 2002; Klimesch et al., 2000) whereas during actual task performance, low power is related to good performance (e.g., Doppelmayr et al., 2005; Klimesch et al., 1997). Moreover, there are also clinical studies which provide evidence supporting the view that alpha-rhythms are relevant for inhibiting irrelevant information (for a review see Klimesch et al., 2007). We therefore investigated these different frequency bands (i.e., delta, theta and different frequencies within the alpha range) to elucidate, which of the frequency bands may mostly be affected by FCA-dependent differences in the efficacy of response inhibition processes.

Materials and methods

Subjects

Thirty neurologically healthy volunteers (15 male and 15 female) with a mean age of 24.4 years (range 20–34) participated in the present study. Handedness was tested with the Edinburgh handedness inventory (Oldfield, 1971). This questionnaire yields a laterality quotient with a range between +100 and −100, with positive values indicating right handedness and negative values left handedness. All participants were right-handed (mean laterality quotient 93.78; range 62.50–100). They gave written informed consent and were treated in accordance with the declaration of Helsinki. The study was approved by the Ethics Committee, Ruhr-University of Bochum.

Experimental paradigm

A Go/Nogo task was used to measure response inhibition to verbal stimuli that were presented tachistoscopically on a 17 inch CRT computer monitor. Participants had to react to 'Go'-stimuli by pressing a key on a custom-made reaction-pad with the index finger of their dominant right hand and to refrain from pressing the key after a 'Nogo'-stimuli was presented. The word 'DRÜCK' (German for 'press') was used as 'Go'-stimulus, whereas the word 'STOPP' (German for 'stop') was used as 'Nogo'-stimulus (Beste et al., 2010c). Overall, the experiment consisted of 640 trials, with 440 of the trials being 'Go' and 200 being 'Nogo' trials. In half of the trials stimuli were presented in the left visual field (LVF), in the other half in the right visual field (RVF). At the beginning of the experiment, participants were instructed to place the head on a chin rest placed at a distance of 57 cm from the monitor. Under this condition 1 cm on the screen represents 1° of visual angle. Subjects had to fixate a black fixation cross that was presented in the middle of the screen throughout the experiment. Each trial started with the tachistoscopic presentation of the stimulus for 185 ms. Afterwards, the central fixation cross was presented for 365 ms. Time pressure was administered by asking participants to react within this 550 ms time period after the stimulus first appeared (Beste et al., 2009b). The inter-trial interval was randomised between 850 and 1050 ms. Only the central fixation cross was presented during this interval.

EEG recording and analysis

During the task the EEG was recorded from 65 Ag–AgCl electrodes and standard positions (FCz, FP1, FP2, F7, F3, F4, F8, FC5, FC1, FC2, FC6, T7, C3, Cz, C4, T8, TP9, CP5, CP1, CP2, CP6, TP10, P7, P3, Pz, P4, P8, PO9, O1, Oz, O2, PO10, AF7, AF3, AF4, AF8, F5, F1, F2, F6, FT9, FT7, FC3, FC4, FT8, FT10, C5, C1, C2, C6, TP7, CP3, CPz, CP4, TP8, P5, P1, P2, P6, PO7, PO3, POz, PO4, PO8). Electrode Cz was used as primary reference. The sampling rate of all recordings was 500 samples/s, applying a filter bandwidth 0–80 Hz to the EEG. Electrode impedances were kept below 5 kΩ. Filtering was applied in the band-pass from 0.5 to 20 Hz (48 dB/oct). Before further processing, the filtered data were visually inspected and all trials contaminated by technical artefacts were rejected. Horizontal and vertical eye movements, as well as pulse-artefacts, were then corrected using an independent component analysis (ICA) applying the Infomax algorithm. The ICA was applied to the un-epoched data set. In the epoched data artefact rejection procedures were applied automatically. The rejection criteria were a maximum voltage step of more than 50 μV/ms, a maximal value difference of 200 μV in a 200 ms interval or activity below 0.1 μV. The overall amount of trials rejected by this procedure was below 5% of all trials in each condition and each EEG-channel.

To achieve a reference-free evaluation, all data analyses (peak and latency quantification) were performed after calculation of current source density (CSD) of the signals (Perrin et al., 1989). The CSD transform replaces the potential at each electrode with the current source density, thus eliminating the reference potential. The algorithm applies the spherical Laplace operator to the potential distribution on the surface of the head. Since the potential distribution is only known for the electrodes used, the procedure of spherical spline interpolation is employed to calculate the continuous potential distribution. The exact mathematical procedure is explained in detail in Perrin et al. (1989). For statistical analysis amplitudes were quantified post to filtering relative to a baseline extending from 200 ms before stimulus presentation until stimulus onset. Stimulus-locked averaging was triggered at the time point when the Go or Nogo-stimulus was presented. This time point was set to zero. For the time-domain analysis epochs had a length of 1200 ms (1000 ms post-stimulus presentation). Subsequent to averaging N2 and P3 amplitudes in Go- and Nogo-trials were evaluated relative to baseline using the accurate trials. The choice of electrodes used for amplitude and latency quantification was oriented at the scalp topography of the Nogo-N2 and Nogo-P3 components as revealed by the data. On the basis of the topographies (see Results section) the N2 amplitudes and latencies were quantified at electrodes FCz, Fz and Cz and P3

potentials on Go and Nogo trials were quantified at electrodes FCz and Pz (Beste et al., 2010d).

sLORETA analysis

Based on the above epochs, source localisation was carried out for components that differed between left and right hemispheric stimulation using sLORETA (Pascual-Marqui, 2002). LORETA (Pascual-Marqui et al., 1999) is a tomographic technique that gives a single solution to what is known as the inverse problem of location of cerebral sources (Marco-Pallares et al., 2005). sLORETA is a new version of LORETA. The main difference is that sources are estimated on the basis of standardised current density (Pascual-Marqui, 2002) allowing a more precise source localisation than the older LORETA-method (Pascual-Marqui, 2002). The intracerebral volume is partitioned in 6239 voxels at 5 mm spatial resolution. Briefly, sLORETA calculates the standardised current density at each of the 6239 voxels in a realistic head model (Fuchs et al., 2002) using the MNI152 template (Mazziotta et al., 2001) with the three-dimensional solution space restricted to cortical gray matter. This calculation is based upon a linear weighted sum of the scalp electric potentials. sLORETA estimates the underlying sources under the assumption that neighbouring voxels should have a maximally similar electrical activity (see also: Fallgatter et al., 2003). The voxel-based sLORETA-images (Pascual-Marqui, 2002) were compared between the stimulation condition in the left and right visual half-field using the sLORETA-built-in voxel-wise randomisation tests (5000 permutations) based on statistical non-parametric mapping (SnPM) (for details see: Holmes et al., 1996), corrected for multiple comparisons. In the current study, the voxels with significant differences ($p<0.01$) were located in specific brain regions with Brodmann areas (BA) and MNI coordinates being provided. sLORETA has mathematically been proven to achieve a reliable localisation of possible underlying sources (Greenblatt et al., 2005; Sekihara et al., 2005). Furthermore sLORETA has been validated in simultaneous EEG/fMRI studies (e.g. Olbrich et al., 2009).

Time–frequency decomposition

For the time–frequency (TF) decomposition epochs were extended ranging from −2000 ms till 2000 ms to allow a reliable measurement of even slow oscillations (e.g. delta frequency band). The time point of stimulus presentation was set to time point zero. The longer epochs for the TF-analysis were constructed to allow a reliable measurement of even slow oscillating components (e.g. delta and theta frequency). TF analysis of the potentials was performed by means of a continuous wavelet transform (CWT) with Morlet wavelets as basis functions after the data was CSD-transformed. In the TF-analysis, the TF energy on stimulus presentation was analysed by means of a modification of a method described previously (e.g., Tallon-Baudry et al., 1997). Complex Morlet wavelets w can be generated in the time domain for different frequencies, f, according to the equation:

$$w(t,f) = A \exp\left(-t^2/2\sigma_t^2\right) \exp\left(2i\pi ft\right),$$

where t is time, $A = \left(\sigma_t\sqrt{\pi}\right)^{-1/2}$, σ_t is the wavelet duration, and $i = \sqrt{-1}$. For analysis and TF-plots, a ratio of $f_0/\sigma_f = 5.5$ was used, where f_0 is the central frequency and σ_f is the width of the Gaussian shape in the frequency domain. The analysis was performed in the frequency range 0.5–20 Hz with a central frequency at 0.5 Hz intervals. For different f_0, time and frequency resolutions can be calculated as $2\sigma_t$ and $2\sigma_f$, respectively. σ_t and σ_f are related by the equation $\sigma_t = 1/(2\pi\sigma_f)$. For example, for $f_0 = 3$ Hz, $2\sigma_t = 425$ ms and $2\sigma_f = 1.5$ Hz; for $f_0 = 5$ Hz, $2\sigma_t = 255$ ms and $2\sigma_f = 2.5$ Hz. TF analysis was performed for both averaged and single-trial RRPs. To obtain total power, after time–frequency decomposition of the single epochs, amplitude values were squared and relevant time–frequency (TF) components were extracted and analysed. A time window of 600 to 800 ms prior to the stimulus onset was used to estimate background activity. The mean of this baseline epoch was subtracted from the TF power measures at each time point of the analysis epoch for each frequency band and electrode. Thus, wavelet power quantification was normalised to the power of the baseline period. To obtain normal distribution of the time–frequency power values, all values were log-transformed (e.g. Beste et al., 2010b, 2007). The TF components that were analysed covered the delta (1.5–3 Hz), theta (4–7 Hz) and alpha (8–12 Hz) frequency bands. The power of the alpha frequency band was quantified its lower (8 Hz), middle (10 Hz) and upper (12 Hz) sub-bands.

Statistics

The behavioural data (i.e. rate of false alarms and reaction times for false alarms in Nogo trials) were analysed using paired samples t-test to compare performance to stimuli presented in the LVF and RVF. The electrophysiological data were analysed using repeated-measures analyses of variance (ANOVAs) with the within-subjects factors electrode (N2: FCz, Fz, Cz; P3: FCz, Pz), condition (Go, Nogo) and visual half-field (RVF, LVF). When appropriate, the degrees of freedom were adjusted using Greenhouse–Geisser correction. All p-levels for post hoc t-tests were adjusted using Bonferroni correction. Effect sizes were given as the proportion of variance accounted for (partial η^2). As a measure of variability, the standard error of the mean (SEM) together with the mean values was given. All statistical analyses were computed by using the software package PASW 18.0.

Results

Behavioural data

In Nogo-trials, the false alarm rate was higher for stimuli that were presented in the LVF (16.4% +/− 1.63) than for stimuli that were presented in the RVF (12.9% +/− 1.28) ($t_{(29)} = 3{,}07$; $p<0.01$). Also, the reaction time for false alarms was shorter for stimuli that were presented in the RVF (335.44 ms +/− 5.51) than for stimuli that were presented in the LVF (357.24 ms +/− 5.94) ($t_{(29)} = 6.45$; $p<0.001$). In Go-trials, the hit rate was in general very high and no difference between the visual fields was observed (LVF: 95.98% +/− 0.77; RVF: 95.86% +/− 0.74; $t_{(29)} = 0.33$; $p=0.74$). Also, the reaction time for correct trials was not significantly different between the visual fields (LVF: 364.04 ms +/− 5.81; RVF: 363.64 ms +/− 5.95; $t_{(29)} = 0.18$; $p = 0.86$).

Neurophysiological data

N2

ERPs on Go- and Nogo-trials for stimulus presentation in the LVF and RVF are shown in Fig. 1A.

As can be seen in the scalp topographies, the topography of the Nogo-N2 was centred around electrodes Fz, FCz and Cz thus revealing a typical N2-topography. Based upon this, the electrodes Fz, FCZ and Cz were chosen for data analysis. For the amplitudes the ANOVA revealed a significant main effect of electrode ($F_{(2,58)} = 8.91$; $p<0.01$; $\eta^2 = 0.24$). The Nogo-N2 was more negative at Fz (−15.55 +/− 1.06) than at FCz (−14.21 +/− 1.58) or Cz (−9.26 +/− 1.85). Moreover a significant main effect of condition emerged ($F_{(1,29)} = 22.21$; $p<0.001$; $\eta^2 = 0.43$), indicating that the N2 was more negative on Nogo-trials (−15.57 +/− 1.43) than on Go-trials (−10.44 +/− 1.26). Furthermore, a significant main effect of visual half-field was observed ($F_{(1,29)} = 5.12$; $p<0.05$; $\eta^2 = 0.15$). The N2 was more negative to stimuli presented in the LVF (−14.14 +/− 1.36) than to stimuli
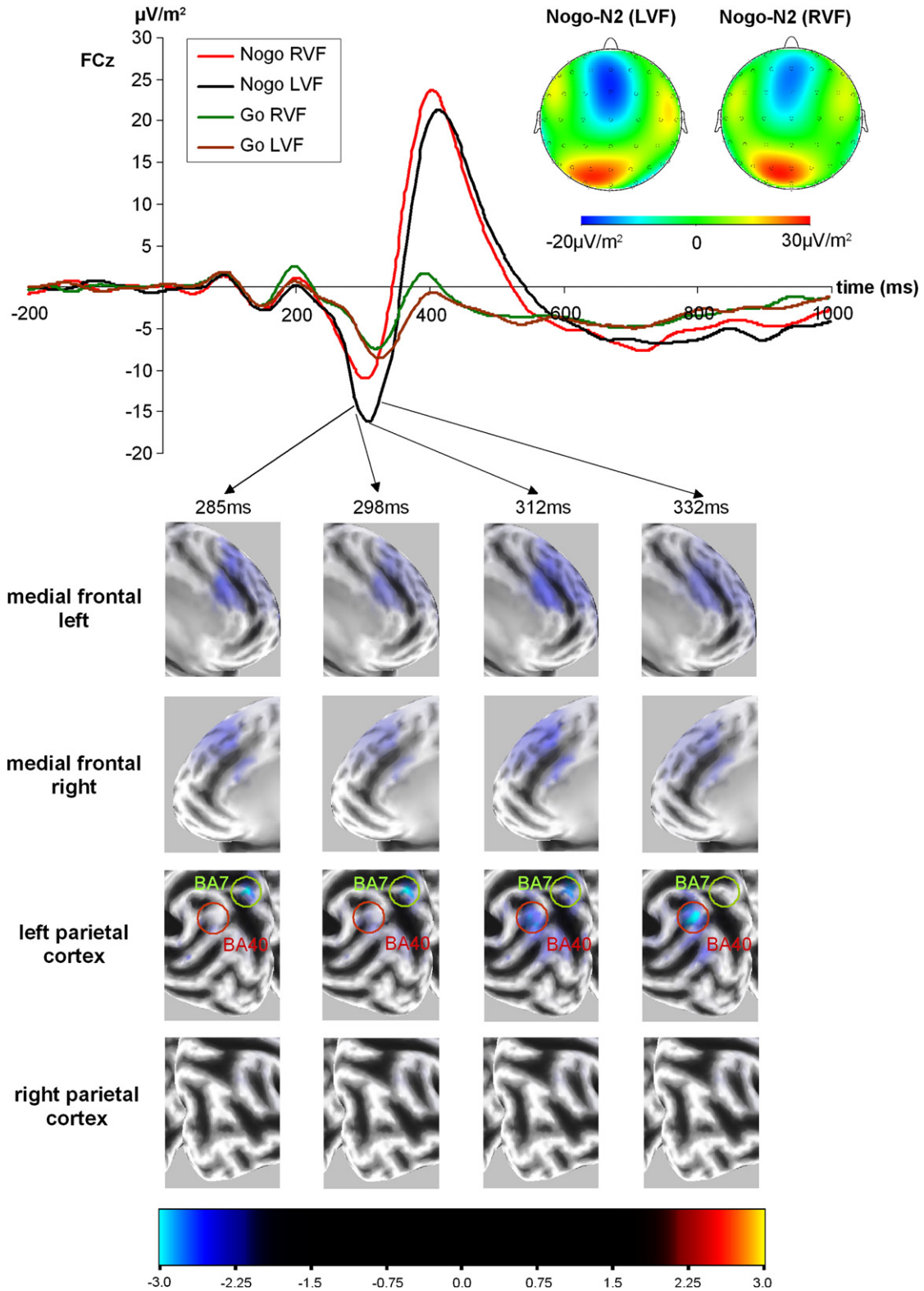
Fig. 1. Upper panel: Time course of ERP components at electrode FCz in the Go and the Nogo condition after stimulus presentation in the LVF and RVF including topographical maps for the Nogo-N2 after stimulus presentation in the LVF and RVF: The time point 0 denotes the point of Go- or Nogo-stimulus presentation. Lower panel: Time course of activation differences in left and right medial frontal and parietal cortices causing the difference in Nogo-N2 amplitudes between presenting stimuli in the LVF and RVF as revealed by sLORETA.

presented in the RVF ($-11.88+/-1.30$). Interestingly, this effect was modulated by the factor condition as revealed by a significant interaction condition×visual half-field ($F_{(1,29)}=8.96$; $p<0.01$; $\eta^2=0.27$). The asymmetry between the visual fields was only significant in Nogo-trials (LVF: $-17.41+/-1.65$; RVF: $-13.74+/-1.47$; post-hoc

test: $p<0.01$) but not in Go-trials trials (LVF: $-10.86+/-1.31$; RVF: $-10.02+/-1.41$; post-hoc test: $p=0.84$). All other main effects and interactions did not reach significance (all $F<1.74$, all $p>0.19$).

For the latencies the ANOVA revealed a significant main effect of electrode ($F_{(2,58)}=24.11$; $p<0.001$; $\eta^2=0.45$). The N2 was prolonged

at Fz (315.60 ms +/− 4.48) compared to FCz (305.65 ms +/− 5.06) and Cz (284.17 ms +/− 5.76). In addition, there was a significant interaction electrode × condition ($F_{(2,58)} = 5.85$; $p < 0.05$; $\eta^2 = 0.17$). At Cz, the N2 latency had a non-significant tendency to be prolonged on Nogo-trials (294.28 ms +/− 5.19) compared to Go-trials (274.07 ms +/− 8.88; post-hoc test: $p = 0.09$). There was no such difference between the conditions at FCz and Fz (both $ps = 1.00$). All other main effects and interactions did not reach significance (all $F < 1.70$, all $p > 0.06$).

P3

For the amplitudes the ANOVA revealed a main effect of electrode ($F_{(1,29)} = 6.03$; $p < 0.05$; $\eta^2 = 0.17$). Overall, the P3 was more positive at Pz (23.05 +/− 2.09) than at FCz (15.22 +/− 2.15). This effect was modulated by an electrode × condition interaction ($F_{(1,29)} = 90.78$; $p < 0.001$; $\eta^2 = 0.76$) that indicated that the P3 was significantly more positive at Pz (24.18 +/− 2.20) than at FCz (4.16 +/− 1.80) on Go-trials (post-hoc test: $p < 0.001$). In contrast, no significant difference in P3 amplitude between Pz (21.92 +/− 2.09) and FCz (26.28 +/− 2.96) was observed on Nogo-trials (post-hoc test: $p = 0.48$).

The ANOVA also revealed a significant main effect of condition ($F_{(1,29)} = 61.92$; $p < 0.001$; $\eta^2 = 0.68$), with the P3 being more positive on Nogo-trials (24.10 +/− 1.81) than on Go-trials (14.17 +/− 1.19). Moreover, a significant interaction condition × visual half-field emerged ($F_{(1,29)} = 5.24$; $p < 0.05$; $\eta^2 = 0.15$). However, this effect was rather weak, since post-hoc tests failed to reach significance for both Nogo- ($p = 0.11$) and Go-trials ($p = 1.00$). All other main effects and interactions did not reach significance (all $F < 2.39$, all $p > 0.07$).

For the latencies the ANOVA revealed a main effect of electrode ($F_{(1,29)} = 66.50$; $p < 0.001$; $\eta^2 = 0.70$), indicating longer Nogo-P3 latencies at FCz (416.80 ms +/− 7.33) than at Pz (376.05 ms +/− 6.06). All other main effects and interactions did not reach significance (all $F < 1.32$, all $p > 0.07$).

sLORETA analysis

For the Nogo-condition, the voxel-based sLORETA-images (6239 voxels at a spatial resolution of 5 mm) (Pascual-Marqui, 2002) were compared between stimulus presentation in LVF versus the RVF using the sLORETA built-in voxel-wise randomisation tests based on statistical non-parametric mapping (SnPM), corrected for multiple comparisons. The voxels with significant differences ($p < 0.01$) were located in the MNI brain. Brodmann areas (BA) as well as coordinates in the MNI-brain were provided by the software (www.unizh.ch/keyinst/NewLORETA/sLORETA/sLORETA.htm). The results of the sLORETA analysis are given in Fig. 1B.

As can be seen in Fig. 1B the difference in Nogo-N2 amplitudes between presenting stimuli in the LVF and RVF was due to differences in activation in the left superior parietal cortex (BA7) and the left inferior parietal cortex (BA40). Moreover, significant voxel cluster were found in the left and right pre-SMA (BA6), medial frontal gyrus (MFG) (BA9) and the anterior cingulate gyrus (ACC) (BA32). In all these areas presentation in the RVF produced less activation than presentation in the LVF.

Time–frequency decomposition

The results of the time–frequency decomposition are given in Fig. 2.

As can be seen in Fig. 2 there was strong increase in total wavelet power in the delta and theta frequency bands in Nogo, compared to Go-trials. For the Nogo-trials, the plots denote differences between left (LVF) and right visual field (RVF) presentation of stimuli especially in the delta frequency band range. However, there was also activation in the sub-delta frequency band in the RVF-condition. Moreover, activity in this frequency band was evident from 400 ms onwards and thus not related to Nogo-N2, which, according to the

time-domain analysis, peaked between 270 and 300 ms after stimulus presentation. The extraction of total wavelet power in the delta and theta frequency bands was therefore confined to this time interval. In the Nogo-condition power in the delta and theta frequency bands was highly correlated (LVF: $r = 0.50$; $p < 0.01$; RVF: $r = 0.37$; $p < 0.05$). Therefore, the delta and theta frequency bands were analysed in separate ANOVAs (see also: Kolev et al., 2010; Beste et al., 2010b).

Delta

For the delta band a 2 × 2 repeated measures ANOVA with the within-subjects factors condition (Go, Nogo) and visual half-field (RVF, LVF) revealed a main effect of condition ($F_{(1,29)} = 24.20$; $p < 0.001$; $\eta^2 = 0.45$) indicating more power in the Nogo-trials (4.16 +/− 0.06) than in Go-trials (3.84 +/− 0.05). A significant interaction condition × half-field ($F_{(1,29)} = 5.15$; $p < 0.05$; $\eta^2 = 0.15$) indicated, that this difference between the conditions was more pronounced in the LVF (Go: 3.79 +/− 0.06; Nogo: 4.22 +/− 0.06; post-hoc test: $p < 0.001$) than in the RVF (Go: 3.88 +/− 0.05; Nogo: 4.09 +/− 0.08; post-hoc test: $p < 0.05$). The main effect of side failed to reach significance ($F_{(1,29)} = 0.09$; $p = 0.77$).

Theta

For the theta band the ANOVA revealed a main effect of condition ($F_{(1,29)} = 82.68$; $p < 0.001$; $\eta^2 = 0.74$) indicating more power in the Nogo-trials (4.25 +/− 0.09) than in Go-trials (3.75 +/− 0.07). All other main effects and interactions did not reach significance (all $F < 2.38$, all $p > 0.13$).

Alpha

For the alpha band a 2 × 2 × 3 repeated measures ANOVA with the within-subjects factors condition (Go, Nogo), visual half-field (RVF, LVF) and alpha frequency sub-band (lower, middle and upper) was calculated. The ANOVA revealed a significant main effect frequency band with the power being highest in the lower alpha band (2.99 +/− 0.07) and consecutively lower in the middle (2.64 +/− 0.07) and upper (2.40 +/− 0.07) alpha frequency band ($F_{(2,58)} = 92.20$; $p < 0.001$; $\eta^2 = 0.76$). Moreover, the power was generally higher in Nogo (2.91 +/− 0.08), compared to Go (2.45 +/− 0.08) trials ($F_{(1,29)} = 33.77$; $p < 0.001$; $\eta^2 = 0.54$). This difference between Go and Nogo trials was more pronounced in the lower (Go: 2.68 +/− 0.09; Nogo: 3.30 +/− 0.08; post hoc test $p < 0.001$), and middle (Go: 2.44 +/− 0.09; Nogo: 2.85 +/− 0.08; post hoc test $p < 0.001$) than in the upper (Go: 2.24 +/− 0.08; Nogo: 2.57 +/− 0.08; post hoc test $p < 0.01$) alpha frequency range as indicated by an interaction condition × alpha frequency sub-band ($F_{(2,58)} = 8.77$; $p < 0.01$; $\eta^2 = 0.23$). Moreover, there was a significant interaction condition × half-field ($F_{(1,29)} = 11.86$; $p < 0.01$; $\eta^2 = 0.29$) indicating that the difference between the conditions was more pronounced in the LVF (Go: 2.37 +/− 0.11; Nogo: 3.01 +/− 0.08; post-hoc test: $p < 0.001$) than in the RVF (Go: 2.54 +/− 0.08; Nogo: 2.81 +/− 0.11; post-hoc test: $p < 0.01$). All other main effects and interactions did not reach significance (all $Fs < 0.65$; all $ps > 0.45$).

Discussion

In this study we investigated the modulation of response-related inhibitory processes by functional cerebral asymmetries (FCAs) via ERPs, sLORETA and time–frequency decomposition analysis. On the behavioural level, participants committed fewer false alarms to verbal Nogo stimuli presented in the RVF compared to stimuli presented in the LVF, reflecting the left-hemispheric dominance for the processing of verbal stimuli (Hugdahl, 2000; Corballis, 2003; Hirnstein et al., 2008; Westerhausen and Hugdahl, 2008). Since the reaction time for false alarms was also shorter for stimuli that were presented in the RVF than for those presented in the LVF, this effect is not due to a speed-accuracy trade-off. This is in line with the findings of Measso
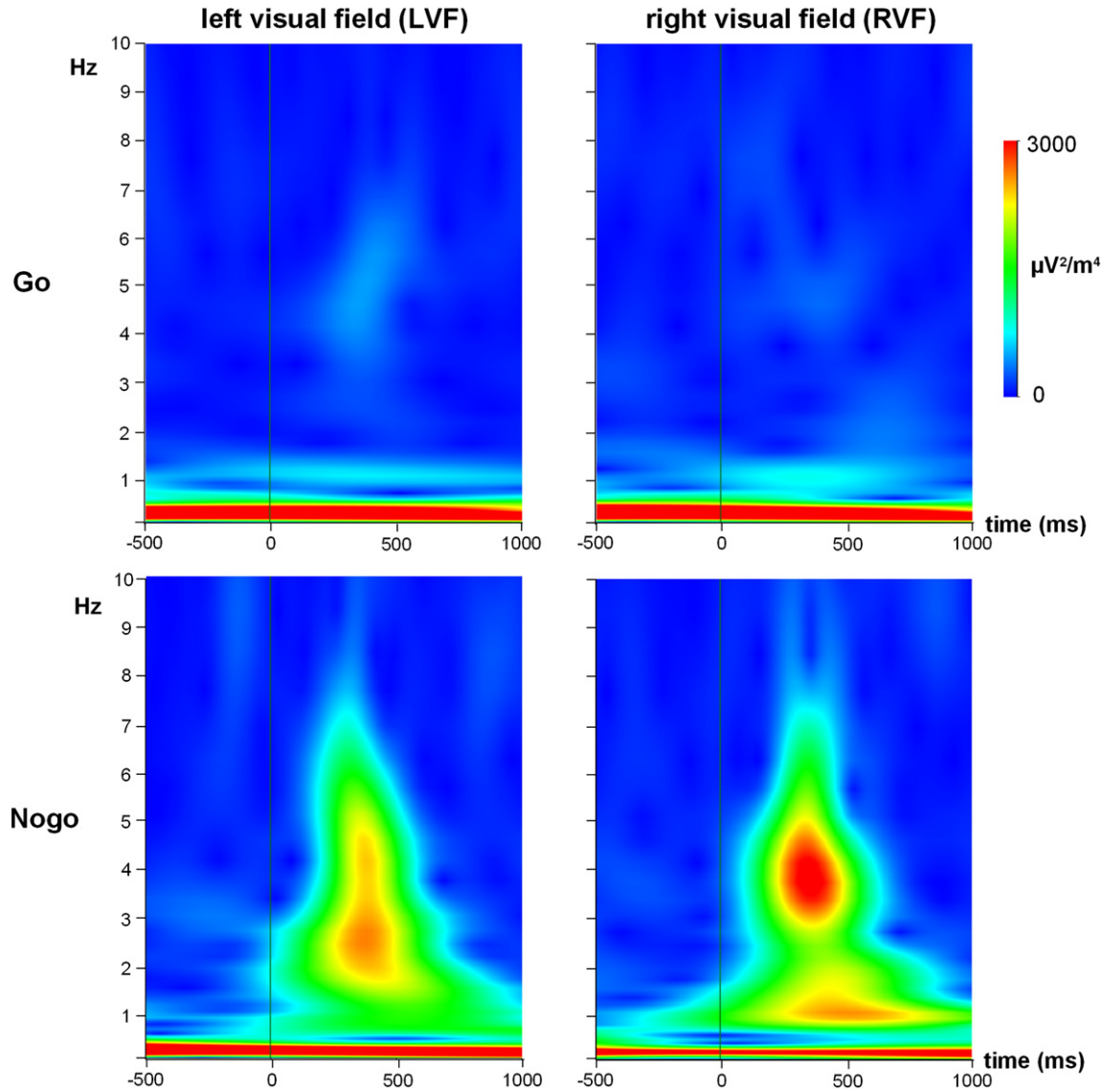
Fig. 2. Total wavelet power in frequency range between 0 and 10 Hz in the Go and the Nogo condition after stimulus presentation in the LVF and RVF. The time point 0 denotes the point of Go- or Nogo-stimulus presentation.

and Zaidel (1990) who also reported a greater efficacy of the left hemisphere in a verbal Go/Nogo task.

In the ERP data, asymmetry effects were observed in the N2 amplitudes, but not in the latencies. We observed an attenuation of the Nogo-N2 when response inhibition was driven by verbal stimuli presented in the RVF compared to the LVF: Since this asymmetry was absent on Go-trials, it specifically reflects the influence of FCAs on inhibition processes and not a general difference between the two hemispheres in Go/Nogo task. Interestingly, the modulation of neuronal processes underlying response inhibition by FCAs is mainly confined to the N2. While the interaction between condition and visual half-field also reached significance for the P3 amplitudes, the variance accounted for by this interaction was only 15% compared to 27% for the N2 amplitude and the post-hoc tests failed to reach significance for both Go- and Nogo-trials. In this regard it has to acknowledge that the unequal frequencies of Go and Nogo trials may bias the P3 (i.e., oddball effects), thus a clear-cut interpretation of this effect is difficult. This confinement of asymmetry effects to the N2 suggests that FCAs modulate specifically those sub-processes of response inhibition that are related to conflict monitoring and/or the efficacy of pre-motor inhibition processes (Falkenstein et al., 1999; Nieuwenhuis et al., 2003).

Using sLORETA, significant voxel cluster were found in the left and right pre-SMA (BA6), medial frontal gyrus (MFG) (BA9) and the ACC (BA32). While the pre-SMA is involved in the selection of action sets (for a review see Rushworth et al., 2004), the MFG plays a critical role in performance monitoring and subsequent adjustments of behaviour (for a review see Ridderinkhof et al., 2004). An involvement of the ACC in response inhibition and its general role in response monitoring functions have been found by a number of studies (van Veen and Carter, 2002; Nieuwenhuis et al., 2003; Ridderinkhof et al., 2004b; Bekker et al., 2005; Yeung and Cohen, 2006; Beste et al., 2008a, 2008b; Wild-Wall et al., 2008; Wascher and Beste, 2010).

The time–frequency analysis shows that during Nogo trials phase-locked frequency band power was increased, compared to Go trials in all examined frequency bands (from delta to alpha). Within the alpha frequency band this difference between conditions was especially expressed in the lower alpha frequency band. The involvement of the alpha frequency band is in accordance with the literature suggesting a role of the alpha frequency band in response inhibition (Klimesch et al., 2007). Moreover, we could show that response inhibition effects are not confined to the alpha frequency band, but were evident in lower frequency bands (delta and theta), too, which fits well to studies in different areas that account for a role of these frequency

bands for general response monitoring processes (e.g. Beste et al., 2010b; Yordanova et al., 2004).

Interestingly, FCAs did only affect the delta and alpha frequency bands, but not the frequencies in the theta band. Moreover, in the alpha band, all three sub-bands are equally affected by FCAs, since only an interaction condition × half-field was observed, but no interaction between frequency sub-bands and these variables was evident. This suggests that the modulatory effects of FCAs on response inhibition and maybe executive functions in general get manifested via very circumscribed frequencies in the lower range, as well as via a broader frequency spectrum in the alpha band.

The above findings suggest that functional cerebral asymmetries strongly modulate the efficacy of response inhibition processes and parietal areas (BA7 and BA40) seem hereby to play an important role. In these areas, differences between left and right hemispheric stimulation were even stronger than in frontal areas (as indicated by t-values of the sLORETA), and also the temporal dynamics were different: Before the peak of the Nogo-N2 (see Fig. 1B) activation differences between left and right hemispheric stimulus presentation were observed in BA7. At the peak of the Nogo-N2, condition-dependent differences in activation became also evident in BA40 and remained there, while activation differences in BA7 subsequently disappeared. In frontal regions no such changes were evident.

Several studies suggest that BA7 gets activated whenever incoming information is complex, or degraded, but is essential for subsequent behavioural processes (e.g. Fokin et al., 2008; Takeichi et al., 2010). The current results show that BA7 is less activated, when stimuli are presented to the language dominant left (the RVF), compared to the on-dominant right hemisphere (the LFV). It is conceivable that the non-dominant right hemisphere is not sufficiently able to trigger response inhibition using verbal stimuli. Therefore this information has to be transferred to the dominant left hemisphere. This could be mediated via the posterior parietal cortex (BA7) which may in turn trigger BA40. Brodmann area 40 is functionally heterogeneous and has been found to be involved in visual word recognition and to contribute to the reading processes (e.g. Stoeckel et al., 2009). Since the left hemisphere is highly specialised for the processing of verbal stimuli the visual word recognition process is less demanding for stimuli presented in the RVF. This leads to less activation in BA40 in the later stages of the inhibition process. In this sense, the increased activation in left BA7 and BA40 may constitute compensatory processes to ensure effective response inhibition. This interpretation is in line with a recent study by Gothelf et al. (2007) in which significantly greater activation in both of these areas during response inhibition was evident in subjects having deficits in several aspects of cognitive control and conflict monitoring (Bish et al., 2005).

When interpreting the results of the present study, it has to be noted that, while it is likely that the effects are caused by the left hemispheric dominance for verbal information processing, other explanations might also be possible. To rule out such alternative explanations (e.g. a hypothetical left hemispheric dominance for response inhibition) it would be an interesting follow-up study to run an experiment in which the participants have to perform a Go/Nogo-task with the same stimuli as in the present study but are asked to analyse spatial instead of verbal aspects of the stimuli. Alternatively, an experiment may be conceived in which participants have to react to spatial stimuli (e.g. complex abstract figures). If the effects observed in the present study would disappear in such spatial Go/Nogo task, it would make a strong argument for the interpretation that the effects are indeed caused by the left hemispheric dominance for verbal information processing.

In summary, functional cerebral asymmetries affect response inhibition functions related to conflict monitoring that are mediated by bilateral medial-prefrontal and left parietal networks. Importantly, the study further shows that asymmetries in behavioural performance

do not necessarily reflect differences in the overall capability of one hemisphere to solve a certain task. Instead, after initial segregated sensory processing, both hemispheres interact to ensure efficient performance. This suggests that even though information is initially confined to one hemisphere, this does not primarily cause behavioural asymmetries. Instead, hemispheric dominances in information processing can induce differences in demands on cognitive processes operating via bilateral networks that ultimately drive behavioural asymmetries.

References

Band, G.P., van Boxtel, G.J., 1999. Inhibitory motor control in stop paradigms: review and reinterpretation of neural mechanisms. Acta Psychol. 101, 179–211.

Bekker, E.M., Kenemans, J.L., Hoeksama, M.R., Talsma, D., Verbaten, M.N., 2005. Source analysis of the N2 in a cued Go/NoGo task. Brain Res. Cogn. Brain Res. 22, 221–231.

Beste, C., Saft, C., Yordanova, J., Andrich, J., Gold, R., Falkenstein, M., Kolev, V., 2007. Functional compensation or pathology in cortico-subcortical interactions in preclinical Huntington's disease. Neuropsychologia 45, 2922–2930.

Beste, C., Saft, C., Andrich, J., Gold, R., Falkenstein, M., 2008a. Response inhibition in Huntington's disease — a study using ERPs and sLORETA. Neuropsychologia 46, 1209–1297.

Beste, C., Saft, C., Andrich, J., Gold, R., Falkenstein, M., 2008b. Stimulus-response compatibility in Huntington's disease: a cognitive-neurophysiological analysis. J. Neurophysiol. 99, 1213–1223.

Beste, C., Dziobek, I., Hielscher, H., Willemssen, R., Falkenstein, M., 2009a. Effects of stimulus-response compatibility on inhibitory processes in Parkinson disease. Eur. J. Neurosci. 29, 855–860.

Beste, C., Willemssen, R., Saft, C., Falkenstein, M., 2009b. Error processing in normal aging and in basal ganglia disorders. Neuroscience 159, 143–149.

Beste, C., Willemssen, R., Saft, C., Falkenstein, M., 2010a. Response inhibition subprocesses and dopaminergic pathways: basal ganglia disease effects. Neuropsychologia 48, 366–373.

Beste, C., Domschke, K., Kolev, V., Yordanova, J., Baffa, A., Falkenstein, M., Konrad, C., 2010b. Functional 5-HT1a receptor polymorphism selectively modulates error-specific subprocesses of performance monitoring. Hum. Brain Mapp. 31, 621–630.

Beste, C., Baune, B.T., Domschke, K., Falkenstein, M., Konrad, C., 2010c. Paradoxical association of the brain-derived-neurotrophic-factor val66met genotype with response inhibition. Neuroscience 66, 178–184.

Beste, C., Baune, B.T., Domschke, K., Falkenstein, M., Konrad, C., 2010d. Dissociable influences of NR2B-receptor related neural transmission on functions of distinct associative basal ganglia circuits. Neuroimage 52, 309–315.

Bish, J.P., Ferrante, S.M., McDonald-McGinn, D., Zackai, E., Simon, T.J., 2005. Maladaptive conflict monitoring as evidence for executive dysfunction in children with chromosome 22q11.2 deletion syndrome. Dev. Sci. 8, 36–43.

Bokura, H., Yamaguchi, S., Kobayashi, S., 2001. Electrophysiological correlates for response inhibition in a Go/NoGo task. Clin. Neurophysiol. 112, 2224–2232.

Chudasama, Y., Robbins, T.W., 2006. Functions of frontostriatal systems in cognition: comparative neuropsychopharmacological studies in rats, monkeys and humans. Biol. Psychol. 73, 19–38.

Corballis, M.C., 2003. From mouth to hand: gesture, speech, and the evolution of right-handedness. Behav. Brain Sci. 26, 199–208.

Doppelmayr, M., Klimesch, W., Stadler, W., Pöllhuber, D., Heine, C., 2002. EEG alpha power and intelligence. Intelligence 30, 289–302.

Doppelmayr, M., Klimesch, W., Hödlmoser, K., Sauseng, P., Gruber, W., 2005. Intelligence related upper alpha desynchronization in a semantic memory task. Brain Res. Bull. 66, 171–177.

Falkenstein, M., 2006. Inhibition, conflict and the Nogo-N2. Clin. Neurophysiol. 117, 1638–1640.

Falkenstein, M., Hoormann, J., Hohnsbein, J., 1999. ERP components in Go/Nogo tasks and their relation to inhibition. Acta Psychol. 101, 267–291.

Fallgatter, A.J., Bartsch, A.J., Zielasek, J., Herrmann, M.J., 2003. Brain electrical dysfunction of the anterior cingulate in schizophrenic patients. Psychiatry Res. 124, 37–48.

Fokin, V.A., Shelepin, Y.E., Kharauzov, A.K., Trufanov, G.E., Sevost'yanov, A.V., Pronin, S.V., Koskin, S.A., 2008. Localization of human cortical areas activated on perception of ordered and chaotic images. Neurosci. Behav. Physiol. 38, 677–685.

Fuchs, M., Kastner, J., Wagner, M., Hawes, S., Ebersole, J.S., 2002. A standardized boundary element method volume conductor model. Clin. Neurophysiol. 113, 702–712.

Garavan, H., Ross, T.J., Murphy, K., Roche, R.A., Stein, E.A., 2002. Dissociable executive functions in the dynamic control of behavior: inhibition, error detection, and correction. Neuroimage 17, 1820–1829.

Gothelf, D., Hoeft, F., Hinard, C., Hallmayer, J.F., Stoecker, J.V., Antonarakis, S.E., Morris, M.A., Reiss, A.L., 2007. Abnormal cortical activation during response inhibition in 22q11.2 deletion syndrome. Hum. Brain Mapp. 28, 533–542.

Greenblatt, R.E., Ossadtchi, A., Pflieger, M.E., 2005. Local linear estimators for the bioelectromagnetic inverse problem. IEEE Trans. Signal Process. 53, 3403–3412.

Hirnstein, M., Hausmann, M., Güntürkün, O., 2008. The evolutionary origins of functional cerebral asymmetries in humans: does lateralization enhance parallel processing? Behav. Brain Res. 187, 297–303.

Holmes, A.P., Blair, R.C., Watson, J.D.G., Ford, I., 1996. Non-parametric analysis of statistic images from functional mapping experiments. J. Cereb. Blood Flow Metab. 16, 7–22.

Hugdahl, K., 2000. Lateralization of cognitive processes in the brain. Acta Psychol. 105, 211–235.

Klimesch, W., Doppelmayr, M., Pachinger, T., Ripper, B., 1997. Brain oscillations and human memory performance: EEG correlates in the upper alpha and theta bands. Neurosci. Lett. 238, 9–12.

Klimesch, W., Vogt, F., Doppelmayr, M., 2000. Interindividual differences in alpha and theta power reflect memory performance. Intelligence 27, 347–362.

Klimesch, W., Sauseng, P., Hanslmayr, S., 2007. EEG alpha oscillations: the inhibition timing hypothesis. Brain Res. Rev. 53, 63–88.

Knudsen, E.I., 2007. Fundamental components of attention. Annu. Rev. Neurosci. 30, 57–78.

Kolev, V., Beste, C., Falkenstein, M., Yordanova, J., 2010. Error-related oscillations: effects of aging on neural systems for behavioural monitoring. J. Psychophysiol. 23, 664, 216–223.

Konishi, S., Nakajima, K., Uchida, I., Sekihara, K., Miyashita, Y., 1998. No-go dominant brain activity in human inferior prefrontal cortex revealed by functional magnetic resonance imaging. Eur. J. Neurosci. 10, 1209–1213.

Marco-Pallares, J., Grau, C., Ruffini, G., 2005. Combined ICA-LORETA analysis of mismatch negativity. Neuroimage 25, 471–477.

Mazziotta, J., Toga, A., Evans, A., Fox, P., Lancaster, J., Zilles, K., Woods, R., Paus, T., Simpson, G., Pike, B., Holmes, C., Collins, L., Thompson, P., MacDonald, D., Iacoboni, M., Schormann, T., Amunts, K., Palomero-Gallagher, N., Geyer, S., Parsons, L., Narr, K., Kabani, N., Le Goualher, L., Boomsma, D., Cannon, T., Kawashima, R., Mazoyer, B., 2001. A probabilistic atlas and reference system for the human brain: International Consortium for Brain Mapping (ICBM). Philos. Trans. R. Soc. Lond. B Biol. Sci. 356, 1293–1322.

Measso, G., Zaidel, E., 1990. Effect of response programming on hemispheric differences in lexical decision. Neuropsychologia 28, 635–646.

Nieuwenhuis, S., Yeung, N., van den Wildenberg, W., Ridderinkhof, K.R., 2003. Electrophysiological correlates of anterior cingulate function in a go/no-go task: effects of response conflict and trial type frequency. Cogn. Affect. Behav. Neurosci. 3, 17–26.

Olbrich, S., Mulert, C., Karch, S., Trenner, M., Leicht, G., Pogarell, O., Hegerl, U., 2009. EEG-vigilance and BOLD effect during simultaneous EEG/fMRI measurement. Neuroimage 45, 319–332.

Oldfield, R.C., 1971. The assessment and analysis of handedness: the Edinburgh Inventory. Neuropsychologia 9, 97–113.

Pascual-Marqui, R.D., 2002. Standardized low-resolution brain electromagnetic tomography (sLORETA): technical details. Methods Find. Exp. Clin. Pharmacol. 24, 5–12.

Pascual-Marqui, R.D., Lehmann, D., Koenig, T., Kochi, K., Merlo, M.C., Hell, D., Koukkou, M., 1999. Low resolution brain electromagnetic tomography (LORETA) functional imaging in acute, neuroleptic-naïve, first-episode, productive schizophrenia. Psychiatry Res. 90, 169–179.

Perrin, F., Pernier, J., Bertrand, O., Echallier, J.F., 1989. Spherical splines for scalp potential and current density mapping. Electroencephalogr. Clin. Neurophysiol. 7, 184–187.

Ridderinkhof, K.R., Ullsperger, M., Crone, E.A., Nieuwenhuis, S., 2004. The role of the medial frontal cortex in cognitive control. Science 306, 443–447.

Ridderinkhof, K.R., van den Wildenberg, W.P., Segalowitz, S.J., Carter, C.S., 2004b. Neurocognitive mechanisms of cognitive control: the role of prefrontal cortex in action selection, response inhibition, performance monitoring and reward-based learning. Brain Cogn. 56, 129–140.

Roach, B.J., Mathalon, D.H., 2008. Event-related EEG time–frequency analysis: an overview of measures and an analysis of early gamma band phase locking in schizophrenia. Schizophr. Bull. 34, 907–926.

Roche, R.A., Garavan, H., Foxe, J.J., O'Mara, S.M., 2005. Individual differences discriminate event-related potentials but not performance during response inhibition. Exp. Brain Res. 160, 60–70.

Rushworth, M.F., Walton, M.E., Kennerley, S.W., Bannerman, D.M., 2004. Action sets and decisions in the medial frontal cortex. Trends Cogn. Sci. 8, 410–417.

Sauseng, P., Klimesch, W., 2008. What does phase information of oscillatory brain activity tell us about cognitive processes? Neurosci. Biobehav. Rev. 32, 1001–1013.

Sekihara, K., Sahani, M., Nagarajan, S.S., 2005. Localization bias and spatial resolution of adaptive and non-adaptive spatial filters for MEG source reconstruction. Neuroimage 25, 1056–1067.

Stoeckel, C., Gough, P.M., Watkins, K.E., Devlin, J.T., 2009. Supramarginal gyrus involvement in visual word recognition. Cortex 45, 1091–1096.

Takeichi, H., Koyama, S., Terao, A., Takeuchi, F., Toyosawa, Y., Murohashi, H., 2010. Comprehension of degraded speech sounds with m-sequence modulation: an fMRI study. Neuroimage 49, 2697–2706.

Tallon-Baudry, C., Bertrand, O., Delpuech, C., Permier, J., 1997. Oscillatory gamma-band (30–70 Hz) activity induced by a visual search task in humans. J. Neurosci. 17, 722–734.

van Veen, V., Carter, C.S., 2002. The anterior cingulate as a conflict monitor: fMRI and ERP studies. Physiol. Behav. 77, 477–482.

Varela, F., Lachaux, J.P., Rodriguez, E., Martinerie, J., 2001. The brainweb: phase synchronization and large-scale integration. Nat. Rev. Neurosci. 2, 229–239.

Wascher, E., Beste, C., 2010. Tuning perceptual competition. J. Neurophysiol. 103, 1248–1254.

Westerhausen, R., Hugdahl, K., 2008. The corpus callosum in dichotic listening studies of hemispheric asymmetry: a review of clinical and experimental evidence. Neurosci. Biobehav. Rev. 32, 1044–1054.

Wild-Wall, N., Willemssen, R., Falkenstein, M., Beste, C., 2008. Time estimation in healthy aging and neurodegenerative basal ganglia disorders. Neurosci. Lett. 442, 34–38.

Yeung, N., Cohen, J.D., 2006. The impact of cognitive deficits on conflict monitoring. Predictable dissociations between the error-related negativity and the N2. Psychol. Sci. 17, 164–171.

Yordanova, J., Falkenstein, M., Hohnsbein, J., Kolev, V., 2004. Parallel systems of error processing in the brain. Neuroimage 22, 590–602.